

GETaLM: A Generator for Electron Tagger and Luminosity Monitor for electron - proton and ion collisions

Jaroslav Adam

Brookhaven National Laboratory, Upton, United States

Abstract

The study of elastic bremsstrahlung and electron tagging in electron-proton or ion collisions is gaining importance with the planned construction of several experimental facilities focused on deep-inelastic scattering (DIS) measurements. This paper describes a program which generates bremsstrahlung photons in electron-proton and electron-ion interactions as well as scattered electrons in bremsstrahlung processes and in a quasi-real photon approximation to the general DIS process. The effects of electron beam divergence and the spread of the interaction vertex are implemented. The program can be used as an input to simulations of instrumentation for bremsstrahlung photon detection, luminosity measurements, electron tagging, and the determination of the cross sections of corresponding processes.

Keywords: Relativistic bremsstrahlung; Luminosity; Deep inelastic scattering;

PROGRAM SUMMARY

Program Title: GETaLM

Licensing provisions: GNU GPLv3

Programming language: Python

External routines: ROOT

Nature of problem: Photons due to relativistic bremsstrahlung processes are produced in collisions of electrons with protons and with ions. Detection of these bremsstrahlung photons is a promising method for luminosity measurements. The

E-mail address: jaroslavadam299@gmail.com

detection of electrons scattered at small angles will impact these measurements. The program generates the bremsstrahlung photons along with final state electrons in the bremsstrahlung process and in an approximation to general electron-proton scattering.

Solution method: Analytic formulas for the cross sections of the specific processes and the relativistic kinematics are used to generate the photons and scattered electrons. A set of effects imposed by the interacting beams can be applied to the generated particles. The output of the program is created using the ROOT program. Total cross sections are obtained by integrating the specific cross section formulas over a given kinematic region.

Restrictions: Currently the electron and proton (ion) beams are assumed to collide head-on, no crossing angle is considered.

References: <https://github.com/adamjaro/GETaLM> and references in this paper.

1. Introduction

The emission of bremsstrahlung photons in relativistic electron-proton and electron-ion collisions provide a convenient process for the measurement of the luminosity. The photons are emitted at very small angles relative to the direction of the electron beam. Several experimental facilities, the Electron-Ion Collider (EIC) [1], the Large Hadron-Electron Collider [2] and the Electron-Ion Collider in China [3] plan to have dedicated instrumentation to measure luminosity by detecting the bremsstrahlung photons and to tag electrons scattered at small angles. The detection of scattered electrons is also used to constrain the kinematics of DIS processes.

The Generator for the Electron Tagger and Luminosity Monitor (GETaLM), presented here, is based on a set of analytic formulas describing the process dynamics and on relativistic kinematics to create the final bremsstrahlung photons and scattered electrons. A similar simulation package was outlined for the HERA collider [4]. The generator is configured from an INI file and the output contains variables related to a particular process and a complete set of kinematic variables for the final photons and electrons. The implementation is done using the ROOT program [5]. A prototype of GETaLM was already used in the EIC study in Ref. [1].

2. Elastic bremsstrahlung

The first non-vanishing Feynman diagrams for elastic bremsstrahlung are shown in Fig. 1. An incoming electron (positron) of momentum p scatters off the external field of the target particle (proton or nucleus), leaving an electron with a momentum p' and a bremsstrahlung photon of momentum k in the final state.

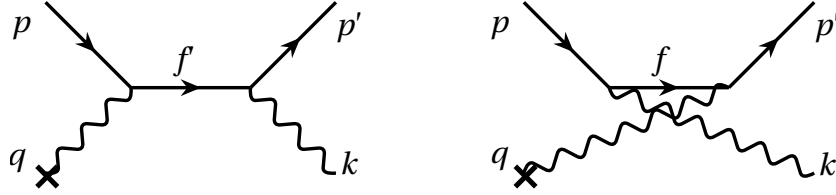


Figure 1: The lowest non-vanishing diagrams for the bremsstrahlung process.

Momentum transfer to the target particle is $q = p' - p + k$, the momenta of intermediate states are $f = p - k$ and $f' = p' + k$.

Several approximations to the process in Fig. 1 which neglect the recoil of the target particle ($q^0 = 0$) are given in the following sections.

2.1. Parameterizations of the bremsstrahlung cross section

The cross section for electron and proton beams of energy E_e and E_p is given by two equivalent parameterizations in Eq. 1 as a function of bremsstrahlung photon energy E_γ [6] and in Eq. 2 as a function of $y = E_\gamma/E_e$ [4].

$$\frac{d\sigma}{dE_\gamma} = 4\alpha r_e^2 \frac{E'_e}{E_\gamma E_e} \left(\frac{E_e}{E'_e} + \frac{E'_e}{E_e} - \frac{2}{3} \right) \left(\ln \frac{4E_p E_e E'_e}{m_p m_e E_\gamma} - \frac{1}{2} \right) \quad (1)$$

$$\frac{d\sigma}{dy} = \frac{4\alpha r_e^2}{y} \left[1 + (1-y)^2 - \frac{2}{3}(1-y) \right] \left[\ln \frac{s(1-y)}{m_p m_e y} - \frac{1}{2} \right] \quad (2)$$

The center-of-mass energy squared is s , the electron and proton rest masses are m_e and m_p . Normalization of the cross section is given by $4\alpha r_e^2 = 2.3179$ mb where α is the fine structure constant and r_e is the classical electron radius.

The angular distribution of bremsstrahlung photons is given by Eq. 3. The angle θ_γ is the angle of the 3-momentum component of the outgoing photon k relative to the 3-momentum component of the incoming electron p .

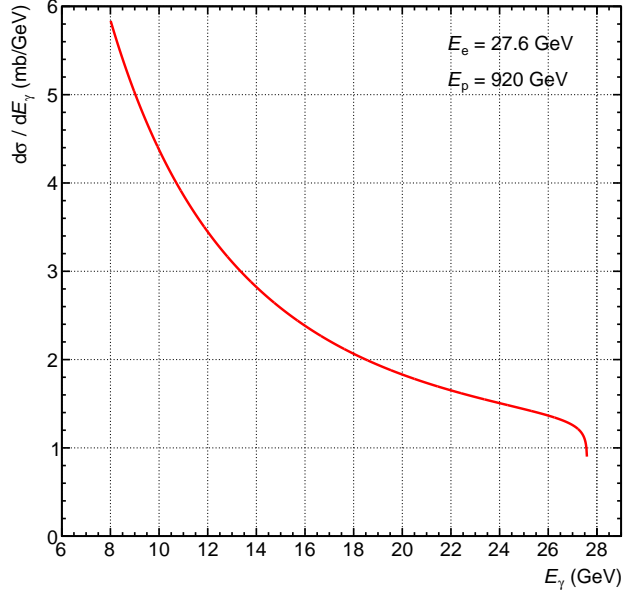


Figure 2: Bremsstrahlung cross section as a function of energy given by Eq. 1.

$$\frac{d\sigma}{d\theta_\gamma} \sim \frac{\theta_\gamma}{((m_e/E_e)^2 + \theta_\gamma^2)^2} \quad (3)$$

The cross section $d\sigma/dE_\gamma$ according to Eq. 1 is shown in Fig. 2 for $E_e = 27.6$ GeV and $E_p = 920$ GeV, an energy corresponding to that of the HERA collider. This result is compatible with a similar calculation in Ref. [7].

2.2. QED calculation in electron-nucleus case

The doubly-differential bremsstrahlung cross section for the general case of a nucleus of electric charge Z is given in Eq. 4 [8].

$$\begin{aligned} \frac{d^2\sigma}{d\omega d\delta} = & 8Z^2\alpha r_e^2 \frac{1}{\omega} \frac{\varepsilon'}{\varepsilon} \frac{\delta}{(1+\delta^2)^2} \times \\ & \times \left\{ \left[\frac{\varepsilon}{\varepsilon'} + \frac{\varepsilon'}{\varepsilon} - \frac{4\delta^2}{(1+\delta^2)^2} \right] \ln \frac{2\varepsilon\varepsilon'}{m_e\omega} - \frac{1}{2} \left[\frac{\varepsilon}{\varepsilon'} + \frac{\varepsilon'}{\varepsilon} + 2 - \frac{16\delta^2}{(1+\delta^2)^2} \right] \right\} \end{aligned} \quad (4)$$

The energy of the bremsstrahlung photon is ω and the electron initial and final energies are ε and ε' respectively, all given in the rest frame of the

target nucleus. The angle of the photon ϑ_γ relative to the initial electron, also in the target nucleus rest frame, is obtained from $\delta = \varepsilon\vartheta_\gamma/m_e$.

The integrated bremsstrahlung cross section for $E_\gamma > 0.1$ GeV σ_{brem} obtained from Eq. 4 is shown in Table 1. The cross sections are evaluated for a set of electron-proton (ep) and electron-gold nucleus (e -Au) energies considered for the EIC.

Species	e	p	e	p	e	Au	e	Au
Energy (GeV)	18	275	5	41	18	110	5	41
σ_{brem}	276.3 mb		159.3 mb		1.563 kb		0.936 kb	

Table 1: Integrated bremsstrahlung cross section σ_{brem} predicted by Eq. 4 for a set of ep and e -Au energies.

The different units of mb and kb for σ_{brem} should be noted in Table 1 reflecting very large bremsstrahlung cross sections in the case of ion beams.

3. Quasi-real photoproduction

The deep inelastic scattering of a lepton of momentum p off a nucleon of momentum P to a final lepton p' and a hadronic system of momentum P_X is shown in Fig. 3.

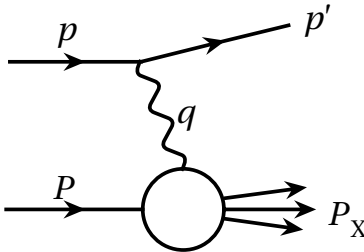


Figure 3: Deep inelastic scattering.

The DIS process is described by three independent kinematic variables. The center-of-mass energy squared is $s = (p+P)^2$, virtuality of the exchanged boson is $q^2 = -Q^2 = (p - p')^2$ and the center-of-mass energy of the boson-nucleon system is $W^2 = (P + q)^2$.

The Bjorken x is $x = Q^2/2Pq$ and inelasticity is $y = Pq/Pp$ giving the fraction of initial lepton energy carried by the exchanged boson. The kinematic variables are related by

$$Q^2 = xys \tag{5}$$

when the rest masses are neglected.

In the approximation to quasi-real photoproduction off protons, where the virtuality Q^2 of the exchanged photon is negligible, the cross section for the process in Fig. 3 is

$$\frac{d^2\sigma}{dxdy} = \frac{\alpha}{2\pi} \frac{1 + (1 - y)^2}{y} \sigma_{\gamma p}(W^2) \frac{1 - x}{x} \tag{6}$$

where $\sigma_{\gamma p}$ is the total photon-proton cross section [9, 10].

The experimental photon-proton cross section is [11]

$$\sigma_{\gamma p}(W^2) = 0.0677 (W^2)^{0.0808} + 0.129 (W^2)^{-0.4525} \text{ (mb)}. \tag{7}$$

Table 2 gives a comparison of the integrated cross section σ_{tot} between the quasi-real approximation in Eq. 6 with $\sigma_{\gamma p}$ from Eq. 7 and the PYTHIA 6 [12] event generator. The comparison is made for a set of electron E_e and proton E_p beam energies considered for the EIC.

Energy (GeV)		σ_{tot} (μb)	
E_e	E_p	Quasi-real	PYTHIA 6
18	275	55.1	54.7
10	100	44.8	40.9
5	41	33.4	28.4

Table 2: Integrated cross section of quasi-real photoproduction and comparison to PYTHIA 6.

The integration range for both the quasi-real and the PYTHIA 6 results is $10^{-11} < x < 1$, $10^{-4} < y < 0.99$, $Q^2 > 10^{-9} \text{ GeV}^2$ and $W > 2 \text{ GeV}$. The actual lower limit on y is imposed by the lower limit on W following the relation $W^2 = ys$ which holds at low Q^2 and when the rest masses are neglected.

4. Particle generation

The formalism outlined in Sec. 2 and Sec. 3 is used to generate the momenta of bremsstrahlung photons, electrons scattered in the bremsstrahlung process and electrons in the final state of quasi-real photoproduction.

4.1. Bremsstrahlung photons from parameterizations

The cross section formulas in Eq. 1 and Eq. 2 are used to obtain the values of bremsstrahlung photon energy E_γ . The energy of the final state electron E'_e in Eq. 1 is set as $E'_e = E_e - E_\gamma$. In the case of Eq. 2, the relation $E_\gamma = yE_e$ is used.

In a similar way, the values of the photon polar angle θ_γ are generated from Eq. 3. Azimuthal angles ϕ_γ are generated as uniform over the full range $0 < \phi_\gamma < 2\pi$.

With a set of values for E_γ , θ_γ and ϕ_γ it is possible to set the photon momentum k in the final state shown in Fig. 1. The final electron momentum is then approximated as $p' = p - k$.

4.2. Bremsstrahlung photons in QED for the electron-nucleus case

Equation 4 is used to simultaneously generate values of photon energy ω and polar angle ϑ_γ given in the rest frame of target nucleus. The relation $\delta = \varepsilon\vartheta_\gamma/m_e$ is used for the polar angle.

The photon azimuthal angles in the nucleus rest frame are generated uniformly over the full range, $0 < \varphi_\gamma < 2\pi$.

The energy ω and angles ϑ_γ and φ_γ are used to set the photon momentum in the nucleus rest frame, which is then boosted to the laboratory frame to obtain the final photon momentum k . As in the previous case the final electron momentum is approximated as $p' = p - k$.

The photon polar angle θ_γ corresponding to a momentum k is no longer independent of its energy E_γ , given the nature of double-differential cross section in Eq. 4. The distribution of the generated photon angles θ_γ and energies E_γ is shown in Fig. 4.

4.3. Electrons in quasi-real photoproduction

The cross section for quasi-real photoproduction in Eq. 6 is transformed to decadic logarithms of Bjorken x and inelasticity y as

$$\begin{aligned} u &= \log_{10}(x) \\ v &= \log_{10}(y) \end{aligned} \tag{8}$$

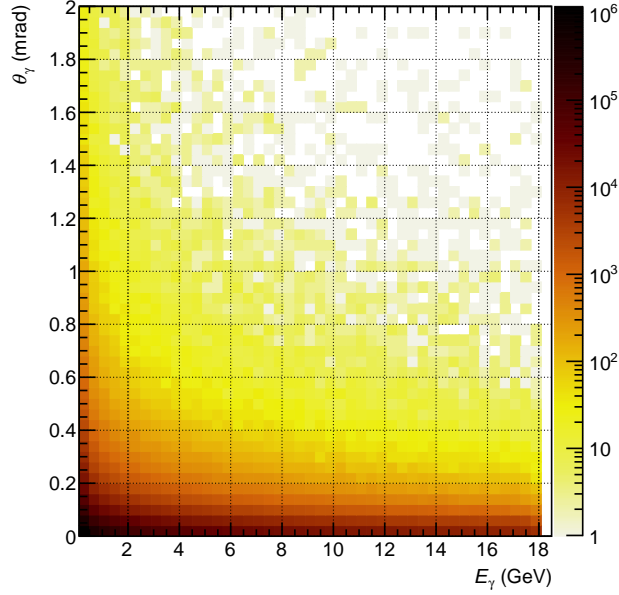


Figure 4: Energy E_γ and polar scattering angle θ_γ of the bremsstrahlung photons for beam energies $E_e = 18$ GeV and $E_p = 275$ GeV.

to increase the precision of generation at low values of x and y .

The values of W^2 at which the photon-proton cross section $\sigma_{\gamma p}$ is evaluated with Eq. 7 are set as $W^2 = ys$, or $W^2 = 10^v s$ after the transformation.

After the transformation in Eq. 8 the cross section Eq. 6 becomes

$$\frac{d^2\sigma}{dudv} = \frac{\alpha}{2\pi} [1 + (1 - 10^v)^2] \cdot \sigma_{\gamma p}(10^v s) \cdot (1 - 10^u). \quad (9)$$

Values for x and y are generated from Eq. 9 and the inverse of Eqs. 8, then the momentum of the scattered electron is found in the proton rest frame and boosted to the laboratory frame.

To find the scattered electron energy ε' and angle ϑ_e in the proton rest frame the kinematic relations

$$y = (\varepsilon - \varepsilon')/\varepsilon \quad (10)$$

$$Q^2 = 4\varepsilon\varepsilon' \sin^2 \frac{\vartheta_e}{2} \quad (11)$$

are used. ε is the initial electron energy in the proton rest frame.

With Eqs. 5 and 10 ϑ_e can be expressed as a function of x and y alone as

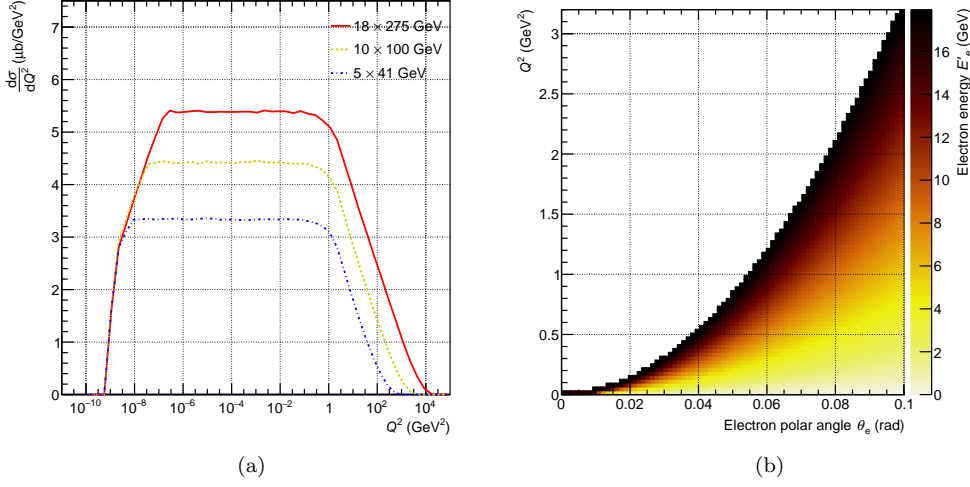


Figure 5: Total cross section of quasi-real photoproduction as a function of Q^2 for several beam energies (a) and the relation between Q^2 , θ_e and E'_e for beam energies $E_e = 18$ GeV and $E_p = 275$ GeV (b).

$$\vartheta_e = 2 \arcsin \left(\frac{1}{2} \sqrt{\frac{xy s}{(1-y)\varepsilon^2}} \right). \quad (12)$$

Using the generated values for x and y , the electron energy ε' and angle ϑ_e are obtained from Eq. 10 and Eq. 12 respectively. The electron azimuthal angle in the proton rest frame φ_e is generated uniformly over the full range $0 < \varphi_e < 2\pi$.

The electron momentum in the proton rest frame is constructed from ε' , ϑ_e , φ_e and the electron rest mass m_e . Then it is boosted to the laboratory frame to get the final electron momentum p' in Fig. 3.

The cross section of quasi-real photoproduction corresponding to Table 2 is shown in Fig. 5a as a function of Q^2 , where the Q^2 is determined by Eq. 5.

The relation between Q^2 and the final electron energy E'_e and polar angle θ_e is shown in Fig. 5b with the energy given by the color scale. The initial kinematics for this figure corresponds to the first line of Table 2.

4.4. Effects of vertex spread and beam angular divergence

In colliding beams the position of interaction (the vertex) depends on the actual profile of interacting beams. The result is a spread in the vertex position both along the beams and in the transverse directions.

The generator can create vertex positions following three separate Gaussian distributions for the direction along the beams and in the transverse directions. Each of the distributions are centered at the origin and are described by a specific width.

The angular divergence of the beam amounts to the spread in the initial angles of particles in the beam interacting with the particles of the opposite beam.

The generator implements the divergence of the electron beam by perturbing the 3-momenta of the final particles. Random Gaussian rotations are imposed on the particles' 3-momenta with a width σ_{div} in the x -direction and another in the y -direction.

The effect of the electron beam divergence on the polar angles θ_γ of bremsstrahlung photons (Sec. 4.2) is illustrated in Fig. 6. The bremsstrahlung cross section as a function of photon angle $d\sigma/d\theta_\gamma$ is shown for the case when the divergence is not considered and for the case of the divergence of $\sigma_{\text{div}} = 202 \mu\text{rad}$ in both transverse directions is included.

The electron beam divergence has a strong effect at low values of Q^2 , as illustrated in Fig. 7 for a sample of events of quasi-real photoproduction with $\sigma_{\text{div}} = 202 \mu\text{rad}$ in both transverse directions. The virtuality Q_e^2 determined from the scattered electron as $Q_e^2 = 2E_e E'_E (1 - \cos(\theta_e))$ including the divergence is compared to the true generated Q^2 given by Eq. 5. The correspondence between Q_e^2 and Q^2 is nearly perfect for $Q^2 \gtrsim 10^{-2} \text{ GeV}^2$ but is completely lost at $Q^2 \lesssim 10^{-4} \text{ GeV}^2$.

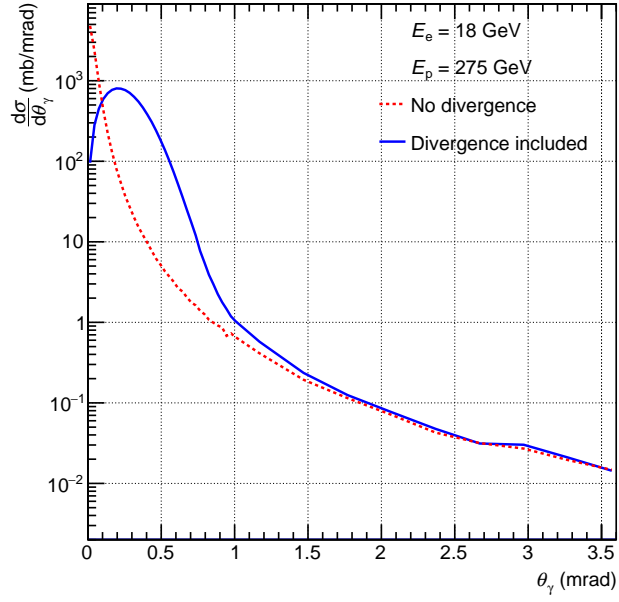


Figure 6: Bremsstrahlung cross section as a function of photon polar angle θ_γ with an illustration of the effect of beam angular divergence.

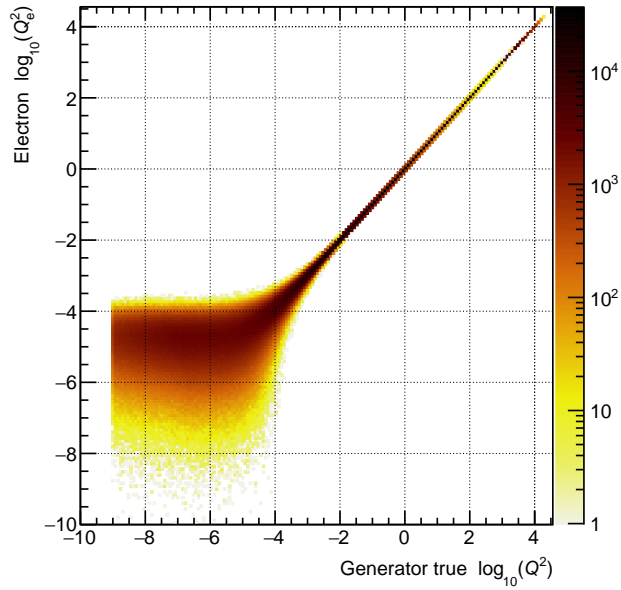


Figure 7: Comparison of Q^2 generated in the event (true Q^2) and Q_e^2 given by the electron kinematics affected by the beam angular divergence.

5. Program flow

The actions carried out by the generator program are described in this section.

- Initialization
 - Configuration is loaded from the input steering card, provided by the user.
 - One of the physics models in Sec. 2 and Sec. 3 is loaded and initialized.
- Event generation
 - A model-specific method for particle generation is called for the loaded physics model.
 - The model generates the particles according to Sec. 4.
 - Optionally, effects of vertex spread and beam angular divergence are applied to generated particles according to Sec 4.4
- Generator output
 - Event-wide variables, specific to the models are written as numerical values to the event `TTree`.
 - Particles are written as a `TClonesArray` of `TParticle` objects in the event `TTree`. The coordinate convention of [1] is used for the particles, namely that the positive z direction points in the direction of the proton (ion) beam.

6. Description of steering card

The generator is configured from a steering card in the INI file. The file is parsed by the `ConfigParser` module. Parameters related to physics models and generator output are grouped in the `[main]` section, parameters describing effects of vertex spread and beam angular divergence belong to the `[beam_effects]` section. The `[beam_effects]` section is optional. Default values for the parameters are indicated in parenthesis.

- General run options

- **Ee, Ep**: Energy of electron and proton (ion) beam respectively in GeV.
 - **nev**: Number of events to generate.
 - **nam**: Name for the output file. The `.root` extension is appended automatically.
 - **model**: Physics model for particle generation.
- Options for bremsstrahlung models
 - The models are selected by the `model` parameter set to 'zeus' for particle generation based on Eq. 1, 'h1' for Eq. 2 or 'Lifshitz_93p16' for Eq. 4
 - **emin**: Minimum bremsstrahlung photon energy E_γ in GeV
 - **tmax**: Maximum photon polar angle θ_γ in rad, available only for 'zeus' model (1.5×10^{-3} rad).
 - **A, Z**: Target nucleus, available only for 'Lifshitz_93p16' model ($A = 1$ and $Z = 1$).
 - **dmax_n**: Maximum value for δ in Eq. 4, the value determines maximum polar angle θ_γ . Available only for 'Lifshitz_93p16' model (100).
 - Options for quasi-real photoproduction
 - The process of quasi-real photoproduction is selected by the `model` parameter set to 'quasi-real'.
 - **xmin, xmax**: Minimum and maximum values for the Bjorken x .
 - **ymin, ymax**: Minimum and maximum values for the inelasticity y .
 - **Q2min, Q2max**: Minimum and maximum values for Q^2 in GeV^2 .
 - **Wmin**: Minimum value for W in GeV, ignored when negative value is set (-1).
 - **Wmax**: Maximum value for W in GeV, ignored when negative value is set (-1).
 - Options for the effects of vertex spread and beam angular divergence

- `sig_x`, `sig_y`, `sig_z`: Width of vertex spread along the x , y and z coordinates respectively.
- `theta_x`, `theta_y`: Width of angular divergence in the x and y coordinates in rad.
- `use_beam_effects`: Value of `true` to apply the effects, `false` otherwise (`false`).

7. Description of test data

The parameters listed in Table 3 were used for Fig. 6, the parameters in Table 4 were used to produce Fig. 5.

```

[main]
Ee = 18
Ep = 275
nev = 5000000
nam = "luminosity"
model = "Lifshitz_93p16"
emin = 0.1
dmax_n = 200
[beam_effects]
use_beam_effects = true
sig_x = 0.119
sig_y = 0.01
sig_z = 9
theta_x = 202e-6
theta_y = 202e-6

```

Table 3: Example steering card for bremsstrahlung photons generation.

```
[main]
Ee = 18
Ep = 275
nev = 5000000
nam = "dis"
model = "quasi-real"
xmin = 1e-11
xmax = 1
ymin = 1e-4
ymax = 0.99
Q2min = 1e-9
Q2max = 1e7
Wmin = 2
```

Table 4: Example steering card for quasi-real photoproduction.

8. Conclusions and outlook

A generator for bremsstrahlung photons and scattered electrons in high energy electron-proton and electron-ion collisions was presented in this paper. It is ready to be used in studies of instrumentation related to luminosity measurements via the detection of the bremsstrahlung photons, as well as studies of dedicated detectors for electrons scattered at small angles.

Its potential application extends to the determination of beam losses due to bremsstrahlung emission and as a fast generator for final state electrons in deep inelastic scattering.

New development is foreseen to incorporate more precise physics models and the effects of a non-negligible crossing angle of the electron and proton (ion) beams. Moreover, the generator illustrates the feasibility of using Python for event generators in the field of high energy physics.

Acknowledgements

The author wishes to thank BNL colleagues for invaluable comments and suggestions. The author acknowledges support from the U.S. Department of Energy under contract number de-sc0012704.

References

- [1] R. Abdul Khalek, et al., Science Requirements and Detector Concepts for the Electron-Ion Collider: EIC Yellow Report (3 2021). [arXiv:2103.05419](#).
- [2] P. Agostini, et al., The Large Hadron-Electron Collider at the HL-LHC (7 2020). [arXiv:2007.14491](#).
- [3] D. P. Anderle, et al., Electron-Ion Collider in China (2 2021). [arXiv:2102.09222](#).
- [4] S. Levonian, H1LUMI - A Fast Simulation Package for the H1 Luminosity System, unpublished H1 note, H1-04/93-287 (1993).
- [5] R. Brun, F. Rademakers, ROOT: An object oriented data analysis framework, Nucl. Instrum. Meth. A 389 (1997) 81–86. [doi:10.1016/S0168-9002\(97\)00048-X](#).
- [6] T. Haas, V. Makarenko, Precision calculation of processes used for luminosity measurement at the ZEUS experiment, Eur. Phys. J. C 71 (2011) 1574. [arXiv:1009.2451](#), [doi:10.1140/epjc/s10052-011-1574-9](#).
- [7] L. Adamczyk, et al., Measurement of the Luminosity in the ZEUS Experiment at HERA II, Nucl. Instrum. Meth. A 744 (2014) 80–90. [arXiv:1306.1391](#), [doi:10.1016/j.nima.2014.01.053](#).
- [8] Berestetskii V.B., Lifshitz E.M., Pitaevskii L.P., Quantum Electrodynamics, Oxford: Pergamon Press 1982.
- [9] U. Amaldi (Ed.), Study of an ep Facility for Europe DESY, Hamburg, April 2-3, 1979., Vol. 790402, Deutsches Electron Synchrotron / European Committee for Future Accelerators, Hamburg, Germany, 1979.
- [10] S. Frixione, M. L. Mangano, P. Nason, G. Ridolfi, Improving the Weizsacker-Williams approximation in electron - proton collisions, Phys. Lett. B 319 (1993) 339–345. [arXiv:hep-ph/9310350](#), [doi:10.1016/0370-2693\(93\)90823-Z](#).
- [11] A. Donnachie, P. V. Landshoff, Total cross-sections, Phys. Lett. B 296 (1992) 227–232. [arXiv:hep-ph/9209205](#), [doi:10.1016/0370-2693\(92\)90832-0](#).

- [12] T. Sjostrand, S. Mrenna, P. Z. Skands, PYTHIA 6.4 Physics and Manual, JHEP 05 (2006) 026. [arXiv:hep-ph/0603175](https://arxiv.org/abs/hep-ph/0603175), [doi:10.1088/1126-6708/2006/05/026](https://doi.org/10.1088/1126-6708/2006/05/026).